Optimally Sensitive and Adaptive Control Systems

S. D. WEINRICH AND LEON LAPIDUS

Department of Chemical Engineering
Princeton University, Princeton, New Jersey 08540

The sensitivity of optimally controlled systems to parameter variations is examined in this paper. Two general approaches toward compensating for these variations are employed. The first, for open-loop systems, involves augmenting the performance index with sensitivity terms and minimizing this combined index. The second approach, an adaptive-type controller, involves estimating those parameter variations that have caused an observed state deviation, and adjusting the control policy in response to this measurement. Numerical examples applied to continuous, discrete-time, and discrete-staged systems demonstrate the effectiveness of these approaches in adapting the control policy to parameter variations.

In recent years there has been extensive literature dealing with different aspects of optimal control and its applications (*1, 15, 25*). From a chemical engineering point of view however, the reliability of any mathematical model used in such control is probably only an approximation for a real process. Successful application of an optimal control policy calculated from such models requires some means of updating an initial model as time passes; alternatively, one might suggest the general form of a model and assume that deviations between the process and the model are due to variations in a number of characteristic parameters in the model. In the present work we shall investigate the influence of such parameter variations on control policies and the resulting trajectories.

Let us consider that an optimal control policy for a given system has been calculated and is applied to that system. The states of that system will evolve along a trajectory in time, the nominal optimal trajectory. The effects of parameter variations on this trajectory can be manifested in two principal ways: (1) the state trajectory will deviate from the nominal trajectory (trajectory sensitivity); and (2) the performance index will change from that associated with the nominal trajectory (performance index sensitivity).

If the object of control is to bring the state to some desired end point, the first type of response can cause the target to be missed. Otherwise, this can merely alter the trajectory so that it passes through some undesirable region in state space (that is, high temperatures, pressures, etc.). The general aim of reducing trajectory sensitivity is to reduce this dispersion due to parameter variation.

A common approach in this case is to define a time-varying sensitivity coefficient $\boldsymbol{\sigma}(t)$ as the first-order change in the state vector $\mathbf{x}(t)$ due to variations of the parameter $\mathbf{q}$, along some nominal trajectory (*4, 7, 14, 29*):

$$\boldsymbol{\sigma}(t) = \partial\mathbf{x}(t)/\partial\mathbf{q} = \mathbf{x}_q \tag{1}$$

These sensitivity coefficients, which can be generated for any number of parameters, can be treated as ordinary state vectors, and adjoined to $\mathbf{x}$ to form an augmented state $\mathbf{X}$: $(\mathbf{X} = [\mathbf{x}, \boldsymbol{\sigma}]^T)$. Likewise, the original performance index can be augmented to include some positive-definite function of $\boldsymbol{\sigma}$, such as $\boldsymbol{\sigma}^T\mathbf{Q}\boldsymbol{\sigma}$. Increasing the magnitude of $\mathbf{Q}$ will tend to reduce the value of $\boldsymbol{\sigma}$ along the trajectory, thus reducing the first-order sensitivity to parameter variation. Unfortunately, this approach has two major disadvantages: (1) the sensitivity vector ($\boldsymbol{\sigma}$) employed is the open-loop sensitivity, whereas closed-loop control is more preferable; (2) an increase in the performance index to achieve sensitivity reduction will occur even if the system's parameters do not vary.

Deviations in the parameters of any optimally controlled system will also cause a resultant deterioration in optimality (the second response). That is, the nominal control policy, calculated to be optimal for the system with its parameters at their nominal values, will no longer be optimal at deviated values of these parameters. Ideally, one would like to be able to measure the parameters and, as they vary, recalculate the optimal control policy, so that control is always optimal regardless of arbitrary parameter variations. This is known as optimally adaptive control, to be denoted henceforth as OAC. For processes where the parameters can be measured in situ, such an implementation is feasible. However, in most practical situations, the parameter variations can only be inferred through their effects upon the output of the process, and the OAC remains an idealized design objective.

As defined, this OAC would generate that minimal performance index for any set of parameter values. Of course, as parameters vary, the numerical value of this minimal index will also change. This variation of the performance index using the OAC will be denoted as the uncontrollable variation, since for any particular parameter values, the index could be reduced no further by altering the control policy.

In contrast, let us consider the situation where the control policy is open-loop. That is, the control policy, calculated for a nominal set of parameters, will be continually applied to the system irrespective of parameter variations. For every set of parameters (other than nominal) the performance index must be higher than that for the OAC, since a nonoptimal control policy is being applied. The difference between the OAC and open-loop (OPLOOP) performance indices shall be denoted as the controllable variation of the performance index. Thus, in attempting to compensate for parameter variations, the goal is to reduce this controllable portion of the performance index to zero, in spite of unknown parameter variations.

Correspondence concerning this paper should be addressed to Leon Lapidus.

Previous work in this area of sensitivity analysis to parameter variations has been summarized by Chang and Wen (*6*) and by Sobral (*28*). Barnett (*2, 3*) has also discussed many aspects of this problem. Other papers of interest are those of Seinfeld (*26, 27*), dealing with applications to chemical engineering systems; Pagurek (*19, 20*) and Witsenhausen (*32, 33*), dealing with sensitivity of the performance index in both closed- and open-loop systems; Kriendler (*10* to *14*), dealing with many different features of sensitivity; McClamroch (*17, 18*) and Rissanen (*22, 23*), dealing with deterioration of the performance index; Rohrer and Sobral (*24*), dealing with formulating a relative sensitivity as a measure of sensitivity; and Werner and Cruz (*31*) and Kokotovic and co-workers (*9*), dealing with the derivation of an optimally sensitive controller.

In the present paper we shall develop the theory for trajectory sensitivity and for optimally sensitive controllers; in the latter case we shall handle the continuous-time, discrete-time, and discrete-staged systems. Numerical examples, including a six-variable absorber system and a staged biochemical reactor, will be used to illustrate the features of control adaptation to parameter variations.

THEORETICAL DEVELOPMENT

Trajectory Sensitivity

To illustrate certain of the features of trajectory or state sensitivity, we shall consider the linear-quadratic (L-Q) control problem (*1, 15*) (a nonlinear system could be used with simple modifications). The system equation is given in continuous form as

$$\dot{\mathbf{x}}(t) = \mathbf{A}\mathbf{x} + \mathbf{B}\mathbf{u} \qquad (2)$$

or, in discrete sampled form, as

$$\mathbf{x}(k+1) = \boldsymbol{\varphi}\mathbf{x}(k) + \boldsymbol{\Delta}\mathbf{u}(k) \qquad (3)$$

$$k = 0, 1, 2, \ldots$$

The matrices $\boldsymbol{\varphi}$ and $\boldsymbol{\Delta}$ are calculated directly from **A** and **B**. The performance index to be minimized along with (3) is

$$I = \sum_{k=1}^{N} [\mathbf{x}^T(k)\mathbf{Q}\mathbf{x}(k) + \mathbf{u}^T(k-1)\mathbf{R}\mathbf{u}(k-1)] + \mathbf{x}^T(N)\mathbf{S}\mathbf{x}(N) \qquad (4)$$

The motivation and formulation of this normal L-Q control problem are well-established (*15*) and we merely need to say that we seek that $\mathbf{u}^*(t)$ which minimizes I and satisfies (2) or (3).

Now let us assume that the $\boldsymbol{\varphi}$ and $\boldsymbol{\Delta}$ matrices as calculated from **A** and **B** are functions of the two parameters q_1 and q_2. In other words, $\boldsymbol{\varphi} = \boldsymbol{\varphi}(q_1, q_2)$ and $\boldsymbol{\Delta} = \boldsymbol{\Delta}(q_1, q_2)$. If these parameters deviate from their original values, then we may write

$$\mathbf{x}(k+1)_{q1} = \boldsymbol{\varphi}_{q1}\mathbf{x}(k) + \boldsymbol{\varphi}\mathbf{x}(k)_{q1} + \boldsymbol{\Delta}_{q1}\mathbf{u}(k) \qquad (5)$$

$$\mathbf{x}(k+1)_{q2} = \boldsymbol{\varphi}_{q2}\mathbf{x}(k) + \boldsymbol{\varphi}\mathbf{x}(k)_{q2} + \boldsymbol{\Delta}_{q2}\mathbf{u}(k) \qquad (6)$$

where $\boldsymbol{\varphi}_{q1}$, $\mathbf{x}(k)_{q1}$, $\boldsymbol{\Delta}_{q1}$, ... indicates differentiation with respect to the subscript variable. Here we have presumed open-loop control and thus $\mathbf{u}(k)_{q1} = \mathbf{u}(k)_{q2} = \mathbf{0}$.

If we define the first-order state sensitivity coefficients $\boldsymbol{\sigma}_1(k) = \mathbf{x}(k)_{q1}$ and $\boldsymbol{\sigma}_2(k) = \mathbf{x}(k)_{q2}$, then (5) and (6) are state equations analogous to (3). Thus we augment the n-dimensional vector **x** with the n-dimensional vectors $\boldsymbol{\sigma}_1$ and $\boldsymbol{\sigma}_2$ to create the $3n$-dimensional vectors $\mathbf{X} = [\mathbf{x}, \boldsymbol{\sigma}_1, \boldsymbol{\sigma}_2]^T$ and convert (3) and (4) to

$$\mathbf{X}(k+1) = \boldsymbol{\Phi}\mathbf{X}(k) + \overline{\boldsymbol{\Delta}}\mathbf{u}(k) \qquad (7)$$

$$\overline{I} = \sum_{k=1}^{N} [\mathbf{X}^T(k)\overline{\mathbf{Q}}\mathbf{X}(k) + \mathbf{u}^T(k-1)\mathbf{R}\mathbf{u}(k-1] + \mathbf{X}^T(N)\overline{\mathbf{S}}\mathbf{X}(N) \qquad (8)$$

where

$$\boldsymbol{\Phi} = \begin{bmatrix} \boldsymbol{\varphi} & 0 & 0 \\ \boldsymbol{\varphi}_{q1} & \boldsymbol{\varphi} & 0 \\ \boldsymbol{\varphi}_{q2} & 0 & \boldsymbol{\varphi} \end{bmatrix} ; \quad \overline{\boldsymbol{\Delta}} = \begin{bmatrix} \boldsymbol{\Delta} \\ \boldsymbol{\Delta}_{q1} \\ \boldsymbol{\Delta}_{q2} \end{bmatrix}$$

$$\overline{\mathbf{Q}} = \begin{bmatrix} \mathbf{Q} & 0 & 0 \\ 0 & \mathbf{Q}_1 & 0 \\ 0 & 0 & \mathbf{Q}_2 \end{bmatrix} ; \quad \overline{\mathbf{S}} = \begin{bmatrix} \mathbf{S} & 0 & 0 \\ 0 & \mathbf{S}_1 & 0 \\ 0 & 0 & \mathbf{S}_2 \end{bmatrix}$$

In the $(3n \times 3n)$ matrices $\overline{\mathbf{Q}}$ and $\overline{\mathbf{S}}$ the diagonal elements $\mathbf{Q}_1$ (and $\mathbf{S}_1$) and $\mathbf{Q}_2$ (and $\mathbf{S}_2$) represent weighting on $\boldsymbol{\sigma}_1$ and $\boldsymbol{\sigma}_2$. The relative magnitude of these matrices reflects the relative weightings of the original performance index and of that applied to the sensitivity terms. The designer may readily examine the trade-off between the original performance index and attainment of sensitivity reduction to select some reasonable compromise between the two. We shall illustrate the explicit features shortly.

Finally we mention a few computational points. The calculation of $\boldsymbol{\varphi}$ and $\boldsymbol{\Delta}$ is known in terms of infinite matrix expansions using certain scaling techniques (*15*). In the present work we need derivatives of these matrices with respect to q; this may be accomplished by a recursion formula which generates succeeding terms in the matrix expansions (*30*). By a proper scaling, convergence to any matrix norm desired may be obtained.

Optimally Sensitive Controller (OSC)

The basic function of the OSC is to provide a feedback law which alters a nominal optimal control policy in response to parameter variations. These variations are inferred through their effects upon measured output states of the system as it evolves in time. The goal is to provide an adaptive-type controller which generates a control policy that is also optimal for the system when its parameters have deviated from their nominal values.

We shall detail the derivation of OSC in a continuous-time domain following Kokotovic (*9*); however, we shall also indicate the discrete-time and discrete-stage forms showing differences as well as equivalences. Consider a system equation of the form

$$\dot{\mathbf{x}}(t) = \mathbf{f}(\mathbf{x}, \mathbf{u}, \mathbf{q}) \qquad \mathbf{x}(0) = \text{given} \qquad (9)$$

or

$$\mathbf{x}(k) = \mathbf{f}_k[\mathbf{x}(k-1), \mathbf{u}(k-1), \mathbf{q}] \qquad (9a)$$

$$k = 1, 2, \ldots,$$

Equation (*9a*) is the discrete-time equivalent of (9); if the index $(k-1)$ is converted to (k) in this and subsequent equations the discrete-staged case is also covered. Alternatively, one may consider the control $\mathbf{u}(k-1)$ acting upon the k^{th} stage of a stagewise system and no revision in nomenclature is needed. The performance index is

$$I = \int_0^{t_f} J(\mathbf{x}, \mathbf{u}, \mathbf{q})dt + K[\mathbf{x}(t_f)] \qquad (10)$$

or

$$I = \sum_{k=1}^{N} J[\mathbf{x}(k), \mathbf{u}(k-1), \mathbf{q}] + K[\mathbf{x}(N)] \qquad (10a)$$

We shall adjoin the n-dimensional state vector with the r-dimensional parameter vector to create an $(n+r)$-dimensional vector $\mathbf{Y} = [\mathbf{x}, \mathbf{q}]^T$. Then (9) may be written as

$$\dot{\mathbf{Y}} = \mathbf{F}[\mathbf{Y}, \mathbf{u}] \qquad \mathbf{Y}(0) = [\mathbf{x}(0), \mathbf{q}^*] \tag{11}$$

with a Hamiltonian

$$H = \boldsymbol{\lambda}^T\mathbf{F}[\mathbf{Y}, \mathbf{u}] + J(\mathbf{Y}, \mathbf{u}) \tag{12}$$

Here $\mathbf{q}^*$ is the nominal set of parameter values. Using the usual necessary conditions of the minimum principle (*1, 21*) and then differentiating with respect to the vector $\mathbf{Y}(0) = [\mathbf{x}(0), \mathbf{q}^*]$, we obtain the linear canonical equations

$$\begin{aligned} \dot{\boldsymbol{\zeta}} &= \mathbf{F_Y}\boldsymbol{\zeta} + \mathbf{F_u}\boldsymbol{\nu} \\ \dot{\boldsymbol{\eta}} &= -H_{\mathrm{YY}}\boldsymbol{\zeta} - \mathbf{F_Y}^T\boldsymbol{\eta} - H_{\mathrm{uY}}\boldsymbol{\nu} \\ 0 &= H_{\mathrm{Yu}}\boldsymbol{\zeta} + \mathbf{F_u}^T\boldsymbol{\eta} + H_{uu}\boldsymbol{\nu} \end{aligned} \tag{13}$$

where

$$\boldsymbol{\zeta} = \mathbf{Y}_{\mathrm{Y(0)}}; \; \boldsymbol{\eta} = \boldsymbol{\lambda}_{\mathrm{Y(0)}} \text{ and } \boldsymbol{\nu} = \mathbf{u}_{\mathrm{Y(0)}}$$

Also

$$\begin{aligned} \boldsymbol{\zeta}(k) &= \mathbf{F_Y}\boldsymbol{\zeta}(k-1) + \mathbf{F_u}\boldsymbol{\nu}(k-1) \\ \boldsymbol{\eta}(k-1) &= H_{\mathrm{YY}}\boldsymbol{\zeta}(k-1) + \mathbf{F_Y}^T\boldsymbol{\eta}(k) + H_{\mathrm{uY}}\boldsymbol{\nu}(k-1) \\ 0 &= H_{\mathrm{Yu}}\boldsymbol{\zeta}(k-1) + \mathbf{F_u}^T\boldsymbol{\eta}(k) + H_{\mathrm{uu}}\boldsymbol{\nu}(k-1) \end{aligned} \tag{13a}$$

The free canonical equations follow by solving for $\boldsymbol{\nu}$ in the last equation of (13) and substituting into the first two equations. This yields, with

$$\overline{\mathbf{A}} = \mathbf{F_u}H_{\mathrm{uu}}^{-1}\mathbf{F_u}^T, \; \overline{\mathbf{F}} = \mathbf{F_Y} - \mathbf{F_u}H_{\mathrm{uu}}^{-1}H_{\mathrm{Yu}},$$

$$\overline{\mathbf{Q}} = H_{\mathrm{YY}} - H_{\mathrm{uY}}H_{\mathrm{uu}}^{-1}H^T_{\mathrm{uY}}$$

$$\begin{aligned} \dot{\boldsymbol{\zeta}} &= \overline{\mathbf{F}}\boldsymbol{\zeta} - \overline{\mathbf{A}}\boldsymbol{\eta} \\ \dot{\boldsymbol{\eta}} &= -\overline{\mathbf{Q}}\boldsymbol{\zeta} - \overline{\mathbf{F}}^T\boldsymbol{\eta} \end{aligned} \tag{14}$$

with initial condition

$$\boldsymbol{\zeta}(0) = \mathbf{I}$$

and final condition

$$\boldsymbol{\eta}(t_f) = K_{\mathrm{YY}}\boldsymbol{\zeta}(t_f) \tag{15}$$

In the same manner

$$\begin{aligned} \boldsymbol{\zeta}(k) &= \overline{\mathbf{F}}\boldsymbol{\zeta}(k-1) - \overline{\mathbf{A}}\boldsymbol{\eta}(k) \\ \boldsymbol{\eta}(k-1) &= \overline{\mathbf{Q}}\boldsymbol{\zeta}(k-1) + \overline{\mathbf{F}}^T\boldsymbol{\eta}(k) \end{aligned} \tag{14a}$$

Since (14) and (15) form a linear two-point boundary-value problem, we can decouple the equations with the Riccati transformation:

$$\boldsymbol{\eta} = \mathbf{P}\boldsymbol{\zeta} \tag{16}$$

Differentiation and comparison to (14) show that P must satisfy the Riccati equation.

$$\dot{\mathbf{P}} = -\mathbf{P}\overline{\mathbf{F}} - \overline{\mathbf{F}}^T\mathbf{P} + \mathbf{P}\overline{\mathbf{A}}\mathbf{P} - \overline{\mathbf{Q}} \tag{17}$$

or

$$\mathbf{P}(k-1) = \overline{\mathbf{F}}^T\mathbf{P}(k)[\mathbf{I} + \overline{\mathbf{A}}\mathbf{P}(k)]^{-1}\overline{\mathbf{F}} + \overline{\mathbf{Q}} \tag{17a}$$

with the condition

$$\mathbf{P}(t_f) = K_{\mathrm{YY}} \tag{18}$$

The continuous Riccati equation may be solved by integrating backward in time starting with the known final condition at t_f. The matrices $\overline{\mathbf{A}}$, $\overline{\mathbf{F}}$, and $\overline{\mathbf{Q}}$ have all been evaluated along the nominal trajectory and are known coefficients. By suitable partitioning of the $\mathbf{P}$, $\overline{\mathbf{A}}$, $\overline{\mathbf{F}}$, and $\overline{\mathbf{Q}}$ matrices, (17) may be broken up into two smaller dimensional equations. One of these is the ordinary Riccati equation for solution of the original optimization problem. Thus, if the second-variation method (5) was employed for solution of the nominal trajectory, this equation has already been solved. The other equation is a linear matrix equation with time-varying coefficients, which may easily be solved. However, once $\mathbf{P}$ is calculated from either (17) or from these dual equations, (16) may be substituted into (14) to yield

$$\dot{\boldsymbol{\zeta}} = [\overline{\mathbf{F}} - \overline{\mathbf{A}}\mathbf{P}]\boldsymbol{\zeta} \tag{19}$$

or

$$\boldsymbol{\zeta}(k) = [\mathbf{I} + \overline{\mathbf{A}}\mathbf{P}(k)]^{-1}\overline{\mathbf{F}}\boldsymbol{\zeta}(k-1) \tag{19a}$$

which may be integrated forward in time starting with the initial condition $\boldsymbol{\zeta}(0) = \mathbf{I}$. Partitioning of $\boldsymbol{\zeta}$ as in (20) will yield the state sensitivity matrix $\mathbf{x_q}$.

$$\boldsymbol{\zeta} = \left[\begin{array}{c|c} \mathbf{x}_{\mathrm{x(0)}} & \mathbf{x_q} \\ \hline \mathbf{0} & \mathbf{I} \end{array}\right] \tag{20}$$

Once $\boldsymbol{\zeta}$ has been obtained, $\boldsymbol{\nu}$ can be evaluated through combination of (13) and (16) as

$$\boldsymbol{\nu} = H_{\mathrm{uu}}^{-1}[H_{\mathrm{uY}} + \mathbf{F_u}^T\mathbf{P}]\boldsymbol{\zeta} \tag{21}$$

A similar partitioning of $\boldsymbol{\nu}$ then specifies the desired control sensitivity matrix $\mathbf{u_q}$:

$$\boldsymbol{\nu} = [\mathbf{u}_{x(0)} \mid \mathbf{u_q}]^T \tag{22}$$

In the discrete case the computation is also simplified because of certain null and identity matrices in $\overline{\mathbf{A}}$, $\overline{\mathbf{F}}$, and $\overline{\mathbf{Q}}$. Thus, if we let

$$\overline{\mathbf{A}} = \begin{bmatrix} \mathbf{A}_1 & 0 \\ \mathbf{0} & \mathbf{0} \end{bmatrix}; \overline{\mathbf{F}} = \begin{bmatrix} \mathbf{F}_1 & \mathbf{F}_2 \\ \mathbf{0} & \mathbf{I} \end{bmatrix}; \overline{\mathbf{Q}} = \begin{bmatrix} \mathbf{Q}_1 & \mathbf{Q}_2 \\ \mathbf{Q}_2^T & \mathbf{Q}_3 \end{bmatrix}$$

$$\mathbf{P} = \begin{bmatrix} \mathbf{P}_1 & \mathbf{P}_2 \\ \mathbf{P}_3 & \mathbf{P}_4 \end{bmatrix}$$

Where $\mathbf{A}_1$ and $\mathbf{P}_1$ are $(n \times n)$ and $\mathbf{P}_2$ is $(n \times r)$ then

$$\mathbf{x}(k)_{\mathrm{q}} = [\mathbf{I} + \mathbf{A}_1\mathbf{P}_1]^{-1}\{\mathbf{F}_1\mathbf{x}(k-1)_{\mathrm{q}} + [\mathbf{F}_2 - \mathbf{A}_1\mathbf{P}_2]\} \tag{20a}$$

$$\mathbf{u}(k-1)_{\mathrm{q}} = -H_{\mathrm{uu}}^{-1}\{H_{\mathrm{xu}}\mathbf{x}(k-1)_{\mathrm{q}} + H_{\mathrm{qu}} + \mathbf{f_u}^T[\mathbf{P}_1\mathbf{x}(k)_{\mathrm{q}} + \mathbf{P}_2]\} \tag{21a}$$

Thus by a procedure analogous to the usual second-variation algorithm for normal optimal control systems, we are able to generate the sensitivity coefficients. To use these coefficients in an OSC we will now find a feedback law which matches the OAC to first order as the parameters change. If the optimal trajectory is $\mathbf{u}^*$ associated with $\mathbf{q}^*$ (the nominal trajectory), then we examine neighboring optimal trajectories differing in $\mathbf{q}$. Thus to first order

$$\hat{\mathbf{u}} = \mathbf{u}^* + \mathbf{u_q}\Delta\mathbf{q} \tag{23}$$

$$\hat{\mathbf{x}} = \mathbf{x}^* + \mathbf{x_q}\Delta\mathbf{q} \tag{24}$$

or

$$\hat{\mathbf{u}}(k) = \mathbf{u}^*(k) + \mathbf{u}(k)_{\mathrm{q}}\Delta q \tag{23a}$$

$$\hat{\mathbf{x}}(k) = \mathbf{x}^*(k) + \mathbf{x}(k)_{\mathrm{q}}\Delta\mathbf{q} \tag{24a}$$

Equating $\Delta\mathbf{q}$ in (23) and (24), we can obtain

$$\hat{\mathbf{u}} = \mathbf{u}^* + \mathbf{u_q}\mathbf{x_q}^{-1}[\hat{\mathbf{x}} - \mathbf{x}^*] \tag{25}$$

or, calling $\mathbf{K}_{fb} = \mathbf{u_q}\mathbf{x_q}^{-1}$,

$$\hat{\mathbf{u}} = \mathbf{u}^* + \mathbf{K}_{fb}[\hat{\mathbf{x}} - \mathbf{x}^*] \tag{26}$$

This is a feedback controller which adjusts the control policy in response to measured deviations of the systems output from nominal. The matrix $\mathbf{K}_{fb}$ uses the sensitivity coefficients determined by the previous procedure.

In deriving (26) we have assumed that $\mathbf{x}_q^{-1}$ exists. This requires that the matrix be square and nonsingular. Hence the measured state vector must be of equal dimension to the parameter vector. If more states are available, then we can select any square nonsingular submatrix of the rectangular $\mathbf{x}_q$ matrix for this inversion. Alternatively, if there are less states than parameters, the pseudoinverse may be employed. Werner and Cruz (*31*) have also suggested artificially augmenting the state vector with other dynamic elements (such as integrators) which are dependent upon the system parameters. Measurement of these states would be included when estimating $\Delta \mathbf{q}$ by inversion of (24).

The discrete-time and discrete-stage relations are essentially equivalent with

$$\mathbf{K}_{fb}(k) = \mathbf{u}(k)_q \mathbf{x}(k)^{-1} \quad \text{Discrete-time} \tag{27}$$

$$= \mathbf{u}(k)_q \mathbf{x}(N)_q^{-1} \quad \text{Discrete-stage} \tag{28}$$

However, the last equation is based upon a simplification (*30*). In the discrete-stage case the normal control diagram is shown in Figure 1 for a general N-stage reactor. The output reactor states $\hat{\mathbf{x}}$ are compared to the precalculated states for the nominal trajectory $\mathbf{x}^*$. Any difference between them due to parameter variation is then multiplied by the feedback matrix $\mathbf{K}_{fb}$. The resulting expression $\mathbf{K}_{fb}[\hat{\mathbf{x}} - \mathbf{x}^*]$ serves as a modification to the precalculated nominal control policy $\mathbf{u}^*$. Hopefully, this modified control policy $\hat{\mathbf{u}}$ will be optimal at the existing deviated parameter values. However, in this case changes in $\mathbf{q}$ require a subsequent measurement of the output of every stage. If the parameter vector is considered equal for every stage and only the final stage is actually measured (the problem is analyzed by treating all the stages as a black-box with a single measurement point), then the equations degenerate to the feedback form of (28).

NUMERICAL RESULTS

Trajectory Sensitivity

Here we shall concern ourselves with reducing dispersion of the state trajectory due to parameter variations. We shall presume that the systems output states are unmeasurable and hence only open-loop control can be applied. In calculating this open-loop control policy, we shall attempt to minimize the original performance index

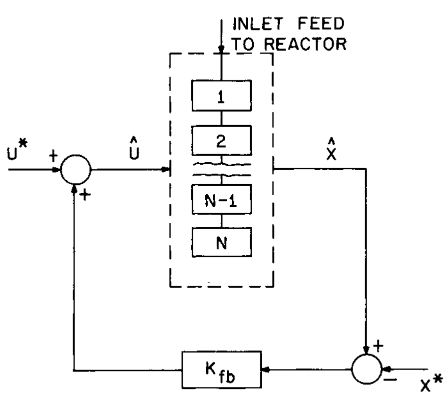

Fig. 1. Schematic diagram of steady state OSC.

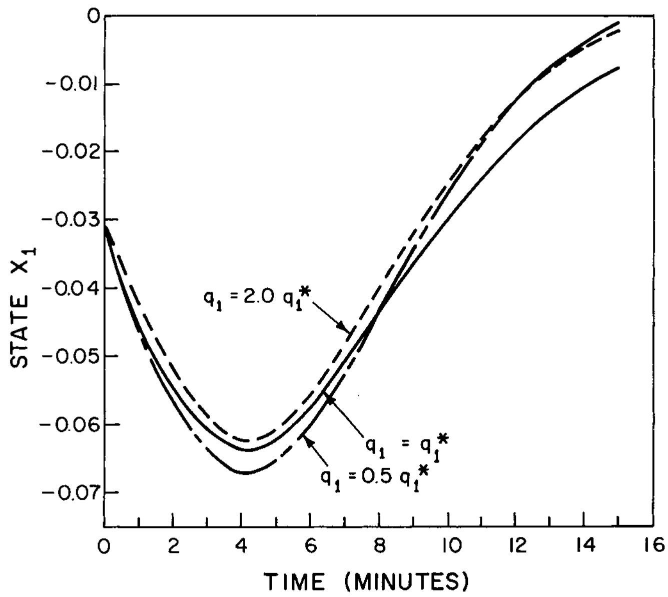

Fig. 2. Dispersion of the state trajectory x_1 due to parameter variations along nominal trajectory for linear absorber. $\omega = 5$. $\mathbf{Q} = \mathbf{R} = \mathbf{I}$, $\mathbf{Q}_2 = \mathbf{S} = \mathbf{S}_1 = \mathbf{S}_2 = \mathbf{0}$. $\mathbf{Q}_1 = \text{diag. } [\omega, 0, 0, 0, 0, 0]$.

while at the same time forcing the system states to move only through regions of state space where they are relatively insensitive to parameter variations.

The system on which we shall test the algorithm is the six-state, two-control absorber described in the literature (*15*). Because the equations have been presented many times, we shall not do so here except to say that they have the form of (2) with

$$\underset{(6 \times 6)}{\mathbf{A}} \equiv \begin{bmatrix} q_2 \text{ on first upper diagonal} \\ -(q_1 + q_2) \text{ on main diagonal} \\ q_1 \text{ on first lower diagonal} \end{bmatrix}$$

$$\underset{(6 \times 2)}{\mathbf{B}} \equiv \begin{bmatrix} q_1 \text{ in left upper corner} \\ q_2 \text{ in right lower corner} \end{bmatrix}$$

The nominal values are $q_1^* = 0.5388$ and $q_2^* = 0.6342$. As in the literature, control is conducted (digitally) over a sampling period of $T = 1.0$ and for $N = 15$ periods [see (3) and (4)].

Because of space limitations we only show here the actual dispersion of the nominal trajectory for x_1 as a result of deviations in q_1 (Figure 2). These results were selected from computer simulations which illustrated the transient evolution of the sensitivity coefficient σ_1 for the nominal and for low sensitivity trajectories using the performance index

$$[\mathbf{Q} = \mathbf{R} = \mathbf{I}, \mathbf{Q}_1 = \text{diag. } [\omega, 0, 0, 0, 0, 0], \quad \mathbf{Q}_2 = \mathbf{0} \text{ and } \overline{\mathbf{S}} = \mathbf{0}]$$

Each sensitivity curve corresponds to a different weighting ω on the first element of $\mathbf{Q}_1$. As this weighting factor increases the state x_1 becomes less and less sensitive to the parameter q_1 over the entire trajectory. These results all show that a considerable reduction of the dispersion along the low sensitivity trajectories can be achieved.

This sensitivity reduction is achieved at the expense of a higher nominal performance index, or cost, of the process. Table 1 presents the performance indices along the undeviated trajectories for increasing values of ω. Keep in mind that although the low sensitivity trajectory is generated by minimization of an augmented performance index (8), the costs, or performance indices, we are re-

Table 1. Variation of the Performance Index for Increasing Sensitivity Weighting

$(\mathbf{Q} = \mathbf{I}, \mathbf{Q}_1 = \text{diag}\ [\omega, 0, 0, 0, 0, 0], \mathbf{Q}_2 = \mathbf{0}, \overline{\mathbf{S}} = \mathbf{0})$

ω	Performance index
0.0	0.1065
1.0	0.1167
2.0	0.1302
5.0	0.1577
10.0	0.1791
25.0	0.1994

Comparison of Nominal and Sensitivity Trajectories for Resistance to Parameter Deviations

$(\mathbf{Q}_1 = \mathbf{I}, \mathbf{Q}_2 = \mathbf{I}, \overline{\mathbf{S}} = \mathbf{0})$

Δq_1, %	Δq_2, %	Nominal, S.S. Dev. ($\times 10^2$)	Sensitivity, S.S. Dev. ($\times 10^2$)
+20	+20	0.3445	0.1659
+20	0	0.1816	0.0840
+50	+50	1.6279	0.7816
+50	−50	4.2306	2.0168
−20	+20	0.7957	0.3513
−20	−20	0.5308	0.2568
0	−50	2.3069	1.1358
−50	−50	4.8497	2.3638

S.S. Dev. = sum of squares deviation of the trajectory.

ferring to, are those for the nominal performance index (4). The contribution due to the additional sensitivity terms in (8) is not considered a true cost, but only a means employed for reducing the system's sensitivity.

Table 1 also illustrates the sensitivity reduction attained for the overall system with respect to variations of both parameters. The weighting matrices employed on the sensitivity terms were $\mathbf{Q}_1 = \mathbf{I}$, $\mathbf{Q}_2 = \mathbf{I}$, and $\overline{\mathbf{S}} = \mathbf{0}$. The overall sum of squares deviation for the low sensitivity case is much less than that for the nominal control, for all parameter deviations examined. The increase in performance index for the undeviated trajectories was from 0.1065 to 0.1893.

All of the above has been related to reducing the sensitivity of the entire trajectory to parameter variations. We have also considered the reduction of the terminal states to parameter variations by inclusion of a non-null $\overline{\mathbf{S}}$ matrix in the formulation. Results (*30*) confirm that one can reduce this form of sensitivity in much the same fashion by including an $\mathbf{S}_1$ matrix in $\overline{\mathbf{S}}$. Furthermore, one can even reduce the sensitivity of the performance index parameter variations by differentiating the index I and augmenting to the original system in essentially the same manner as above.

Thus the state trajectory or performance index sensitivity for open-loop systems may be reduced by the techniques described. One may readily incorporate the sensitivity behavior of the system directly into the selection of its control policy. As a result of this sensitivity reduction however, the performance index, or cost, of the process must increase. This represents a trade-off between optimality (the performance index) and achievement of sensitivity reduction.

Continuous OSC

To illustrate the simplest form of OSC, we have selected two linear-quadratic systems. The first is a scalar CSTR (15) with one-state, one-control, and one-variable parameter; the second is a five-state, five-control, and one-variable parameter system due to Sage (*25*). We will not present the explicit equations but they have the form of (2) and (10).

Turning first to the CSTR case we select a nominal value of the parameter (corresponding to residence time) of $q^* = 1.0$. Since there is only one-state and one-parameter, we have no problem in the inversion of the sensitivity matrices Figure 3 illustrates typical results obtained for $q = 0.90$. Note how the OSC starts at the open-loop value and moves slowly toward the OAC policy as time elapses. This is typical of all results obtained. Of further interest is the value of the performance indices for q ranging from 0.5 to 1.5. There is an approximately 25% decrease in the OAC performance index in this range. This variation is termed the noncontrollable variation of the index, since at each parameter value, no other control policy could reduce the index further. By contrast, the open-loop (OPLOOP) index is calculated with u^* but with the system equations set with q. It is this difference between the OAC and OPLOOP indices, at each parameter value, that we denote as the controllable portion of the performance index, since it can be reduced by employing a better control policy than the OPLOOP one. This is precisely the goal of the OSC.

Next we turn to the system of Sage in which a nominal $q^* = 1.0$ (corresponding to a value of thermal diffusivity) was used. Here a choice exists over which of the five states to measure for feedback for the one parameter. Preliminary calculations showed that the sensitivity of the state x_1 to variations in the parameter q is identical to the negative sensitivity of the state x_5, over the entire trajectory. Hence the use of either of these states for feedback is completely equivalent. Also, due to symmetry, the

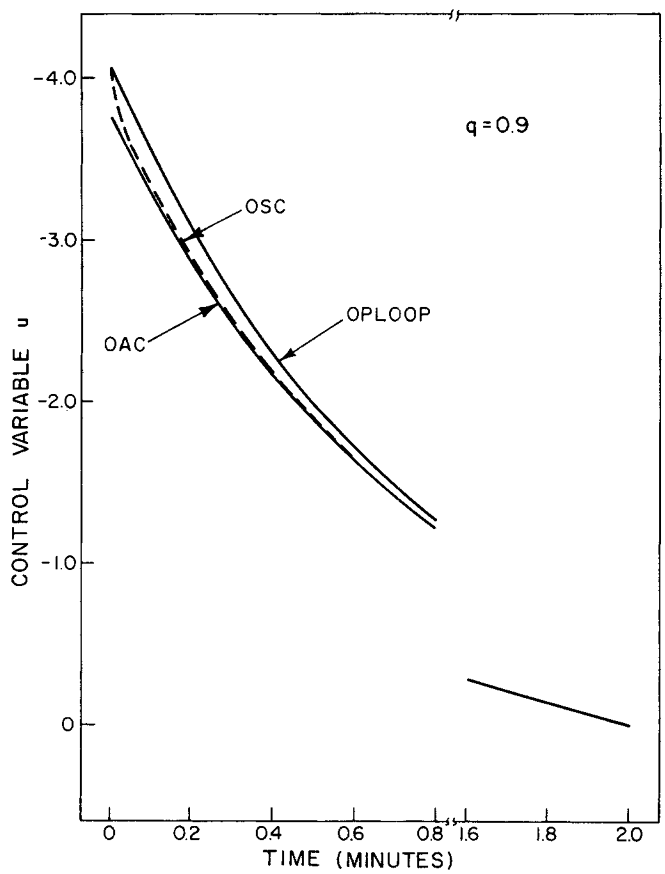

Fig. 3. Calculated control policy for CSTR. $q = 0.9$, $\mathbf{S} = \mathbf{0}$.

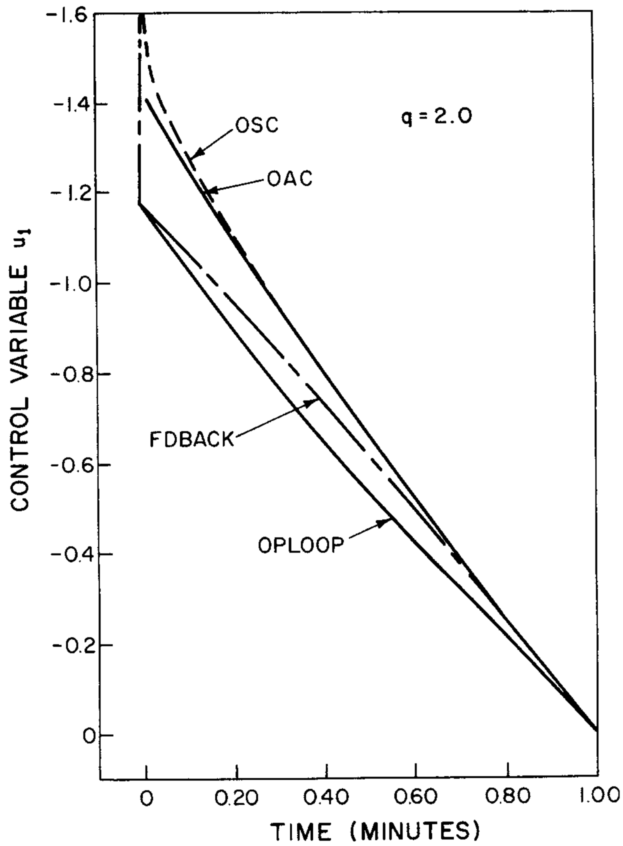

Fig. 4. Calculated control policy for Sage system. $q = 2.0$, $S = 0$. State x_1 measured.

center state (x_3) is completely insensitive to parameter variation. Thus we are led to select either x_1 or x_2 for measurement (or equivalently x_4 or x_5).

Figure 4 shows results typical of the calculations with OSC compared to the linear-quadratic feedback controller (FDBACK), to the OPLOOP, and to OAC for its response to parameter variations. The first element u_1 of the control vector $\mathbf{u}$ is shown for the largest parameter change, an increase of 100%. There is a considerable initial overshoot of the OSC controller but this settles down very quickly and the remaining control policy is almost identical to the OAC. The FDBACK controller, while superior to the open-loop mode, remains distant from the OAC control over most of the trajectory. The corresponding state trajectories also demonstrate the OSC's superiority. Their state trajectories match that for the OAC much closer than do the OPLOOP or FDBACK controllers. The behavior illustrated by these results is typical of the results obtained for all parameter deviations using both $\mathbf{S} = \mathbf{0}$ and $\mathbf{S} = 50\mathbf{I}$. In addition, the performance indices indicate that OSC is superior to the feedback or open-loop control over the entire range of deviations examined.

Discrete-Time OSC

Before discussing the results of the discrete-time OSC, we should point out a significant difference between the continuous and discrete cases. Because of the finite-time period over which the control is applied (the discrete character of this formulation), it is impossible to deviate from the nominal or open-loop control until the first time period has elapsed. To alleviate this problem, one must include the open-loop nature of the trajectory into the generation of the sensitivity matrices. That is, we write the state equation as

$$\mathbf{x}(k+1) = \boldsymbol{\varphi}\mathbf{x}(k) + \boldsymbol{\Delta}\mathbf{v} \quad (29)$$

where $\mathbf{v}$, a constant vector, is equal to the numerical value of the nominal control over the first time step. Hence, in calculating the various derivatives $\mathbf{H}_{ux}$, $\mathbf{H}_{xx}$, $\mathbf{F}_u$, etc., we set all derivatives with respect to $\mathbf{u}$ to zero over this first time interval. The $\mathbf{x}(k)_q$ that one now calculates after this first time interval correctly represents the true open-loop sensitivity and the initial estimation of Δq from ($24a$) will be markedly improved.

This modification was employed for most of the calculated results. Thus, where the term OSC is referred to, it shall be understood that it includes this modifying feature.

The absorber system mentioned previously was used to test this discrete-time OSC algorithm. Other systems such as the batch reactor detailed by Lee (*16*) with parameter variations in the activation energies were also investigated, but we shall not quote these results here.

The calculational procedure was implemented in the following manner:

1. The normal optimization problem was solved with all parameters assumed at their nominal values. For the absorber, a discrete-time method described by Lapidus and Luus (*15*) was employed for this optimization.

2. Once this optimal trajectory was calculated, the required matrices $\mathbf{F}_x$, $\mathbf{H}_{xx}$, $\mathbf{H}_{uu}$, etc., were generated along this trajectory. For the absorber problem, the first and second derivative matrices of $\boldsymbol{\varphi}$ and $\boldsymbol{\Delta}$ with respect to the parameters were calculated by expansion of the exponential and term-by-term differentiation.

3. The algorithm described in the theory section was applied to generate the optimally sensitive feedback matrix $\mathbf{K}_{fb}(k)$ at each time step k, which was stored in computer memory.

4. Control of the system was then begun. Over the first time step, no correction to the nominal control action could be made since the state trajectory had not yet deviated from nominal. However, once $\mathbf{u}^*(0)$ is applied and $\hat{\mathbf{x}}(1)$ is generated from the system equations, the state deviation $[\hat{\mathbf{x}}(1) - \mathbf{x}^*(1)]$ is known and a correction can be applied to the nominal control as given by (26).

The absorber system was operated with variations in both parameters (dual) and the two states measured were x_3 and x_4. Since the absorber is a linear-quadratic system, a closed-loop feedback control law is calculable. The OSC algorithm was compared to this feedback law for its effectiveness in compensating for parameter deviations. Figure 5 compares the control trajectory u_1 for the OSC, OAC, OPLOOP, and FDBACK controllers for a 50% increase in the parameter q_2. The feedback law provides a monotonically decreasing control trajectory approaching the origin. The OSC algorithm, on the other hand, produces trajectories that tend to move toward and merge with the OAC path. The corresponding state trajectory exhibits this same type of behavior.

Generally, for small to moderate (<50%) parameter deviations, the OSC produced a lower performance index than did the feedback control law. Figure 6 illustrates the controllable portion of the performance index as a function of variations in the parameter q_1. These results are typical of those obtained on the absorber system. The OSC is superior to the ordinary feedback controller for all but the largest parameter deviations. For all these cases, the feedback control law, which always tended to bring the system to the origin, could do so by an entirely different path from the OSC or OAC and still not reflect this in its performance index. However, the OSC is much more successful in following the optimally adaptive trajectory.

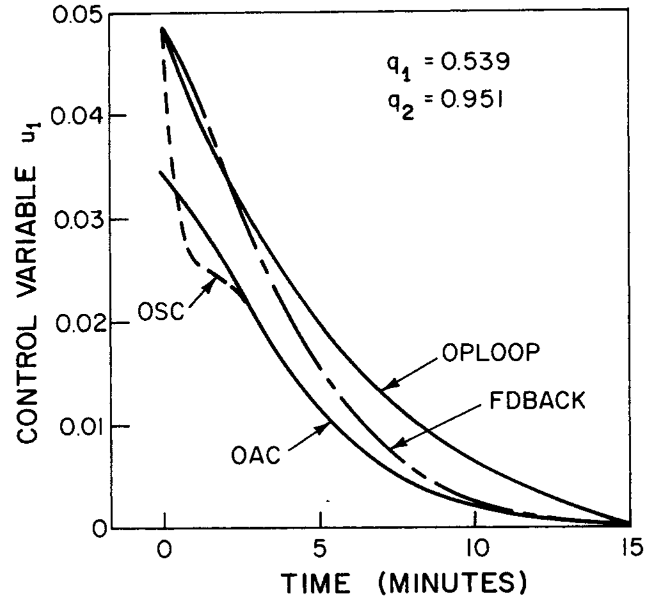

Fig. 5. Control trajectory u_1 for absorber. $q_1^* = 0.539$, $q_2 = 0.951$, $S = 0$. States x_3, x_4 measured.

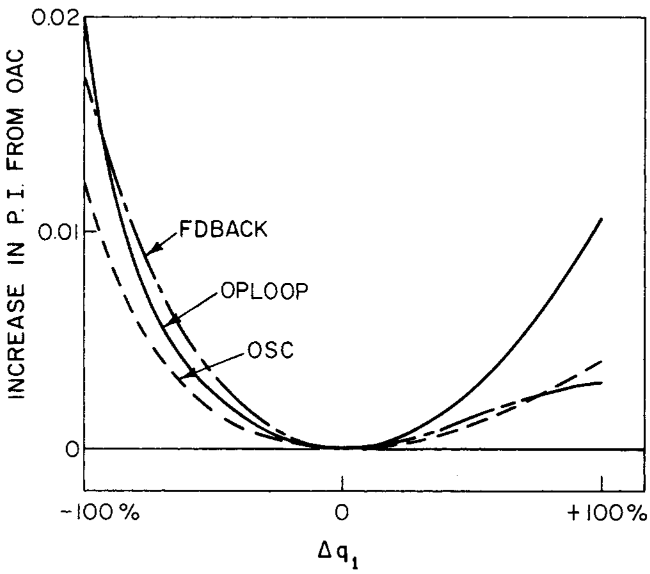

Fig. 6. Variation in controllable portion of performance index for absorber versus q_1. $q_2^* = 0.634$, $S = 0$.

Discrete-Stage OSC

Here we shall illustrate the application of a discrete optimally sensitive controller (OSC) to the steady state feedback control of a three-stage biochemical reactor system. The basic goal is to adjust that constant control policy applied to the reactor system, such that it is always optimal in spite of system parameter variations. A feedback law is implemented that estimates those parameter variations that have caused the output states to deviate from nominal, and adjusts the control policy in light of these variations.

The specific system was originally described by Fan (8). The first-order irreversible reaction

$$A \overset{d}{\rightarrow} E \overset{h}{\rightarrow} C$$

is carried out in a series of three staged reactors of equal residence time θ. The rate constants d and h have been empirically determined as functions of the control variable u. These relations are

$$d(u) = q_1u^2 + 10u + 12$$

$$h(u) = q_2u^2 + 9u - 6$$

Physically, u could represent either the temperature or pH of the reactor. q_1, q_2, and θ will be considered the varying parameters. Their nominal values are -3.0, -1.0, and 0.01, respectively. By a material balance on each stage, the following system equations may be obtained:

$$x_1(k) = x_1(k-1)/[1 + d(k)\theta]$$

$$x_2(k) = \{x_2(k-1) + d(k)x_1(k-1)\theta/[1 + d(k)\theta]\}/[1 + h(k)\theta]$$

$$x_3(k) = x_3(k-1) + h(k)\theta/[1 + h(k)\theta]\{x_2(k-1) + d(k)x_1(k-1)\theta/[1 + d(k)\theta]\}$$

where $x_1(k)$ is the concentration of component x_1 leaving the k^{th} reactor, $d(k) = d[u(k)]$, and $h(k) = h[u(k)]$.

Fan solved the problem of selecting the control variable u for each of the three reactors so as to maximize the yield of component C at the outlet of the third stage. Here, we shall attempt to apply the OSC as an adaptive controller to compensate for both single- and dual-parameter variations of q_1, q_2, and θ. The goal of the OSC is to alter the control variables $u(k)$ as the parameters change to increase the yield of component C at the outlet to its maximum possible value.

The present algorithm employs a feedback matrix $\mathbf{K}_{fb}(k)$, which when acting upon the deviation of the outlet states from nominal, applies a correction to the nominal control. $\mathbf{u}^*(k)$ and $\mathbf{x}^*(N)$ are nominal values (stored in computer memory) and $\hat{\mathbf{u}}(k)$ and $\hat{\mathbf{x}}(N)$ are, respectively, the control applied and the resultant output state of the system.

The calculational procedure was implemented in the following manner:

1. The optimal control policy $\mathbf{u}^*(k)$, $(k = 1, .. N)$ was calculated via the discrete maximum principle with all parameters at their nominal values, as done by Fan.
2. The resultant nominal optimal trajectory $\mathbf{x}^*(k)$, $(k = 1, .. N)$ was generated and stored in memory, along with $\mathbf{u}^*$.
3. The OSC algorithm described in the theory section was applied along this nominal trajectory to generate the optimally sensitive feedback matrix $\mathbf{K}_{fb}(k)$.
4. At this point the control scheme can be applied to the reactor, where parameters can deviate. However, because we are simulating the reactor, a small problem arises, namely, to generate $\hat{\mathbf{u}}(k)$, $\hat{\mathbf{x}}(N)$ the system output, must be known. However, $\hat{\mathbf{x}}(N)$ is unknown until $\hat{\mathbf{u}}(k)$ is applied.

This can be alleviated by choosing an $\hat{\mathbf{x}}(N)$, calculating $\hat{\mathbf{u}}(k)$ and applying it to the system equations (with deviated parameters) to generate a new $\hat{\mathbf{x}}(N)$ and continuing in this manner, until neither showed any change. Since the optimally adaptive values of $\hat{\mathbf{x}}(N)$ and $\hat{\mathbf{u}}(k)$ at these deviated parameters were also calculated for comparison, and since we hope $\hat{\mathbf{x}}(N)$ and $\hat{\mathbf{u}}(k)$ approximate these optimal values, they served as logical starting points for the iteration. This iteration procedure did not always converge however, but occasionally oscillated about the optimally adaptive values with increasing amplitude.

The cause of this instability can be related to the overall gain of the feedback loop. If this gain is too high ($\mathbf{K}_{fb}$ is too large) the resulting correction is so large that the system overshoots its optimal operating condition. The new correction from this latest point drives the system back the other way, again beyond the optimal condition, with deviations from optimality increasing with each swing.

An analysis of this stability problem has been presented (*30*), where necessary and sufficient conditions for guaranteeing stability are obtained. These merely require that the eigenvalues of the overall control loop matrix be less than unity in absolute value.

In compensating for single-parameter deviations, a choice exists over which output state to measure. Where the use of one particular state resulted in instability, the problem could always be alleviated by using a different state for measurement. In fact, measuring component x_3 (which corresponds to the performance index) always resulted in a stable feedback loop.

Even where a state was measured such that the loop was unstable, the system could still be stabilized through a reduction of the feedback gain. If the $\mathbf{K}_{fb}$ matrix is multiplied by some scalar factor w between 0 and 1, such that the eigenvalues (λ) of the overall loop matrix are reduced below unity (in absolute value), stability will be attained. The true optimally sensitive feedback matrix is no longer being applied however, and so there must be a deterioration in optimal performance. This is illustrative of the traditional compromise between accuracy and stability in feedback control systems.

Two factors were used to reduce the gain, each guaranteeing a different margin of stability: $w = 0.90/\max|\lambda|$; $w = 0.75/\max|\lambda|$. In all cases the deterioration of optimal performance with these factors was extremely small. Figure 7 illustrates a few of the results obtained. The performance index using the OSC matches the optimally adaptive one extremely closely over a significant range of parameter deviations. Figure 8 compares the calculated OSC control policy for each stage with the OAC and open-loop controls, for variations of parameter q_1. The state x_3 was measured for feedback. The optimally sensitive control matches the OAC quite well over the parameter range examined. Similar results were obtained for deviations of q_2 and θ. For those cases where the feedback matrix $\mathbf{K}_{fb}$ had to be greatly diminished, there is a small but detectable difference in the calculated control policy. In general, however, these differences had very little effect on the overall performance index for the process. Also, note that on the performance index curve (Figure 7), the OSC follows the OAC much closer over the parameter range than do the control variables of Figure 8. This occurs because at the optimum $I_u = 0$ and thus, near this optimum, the performance index is relatively insensitive to control.

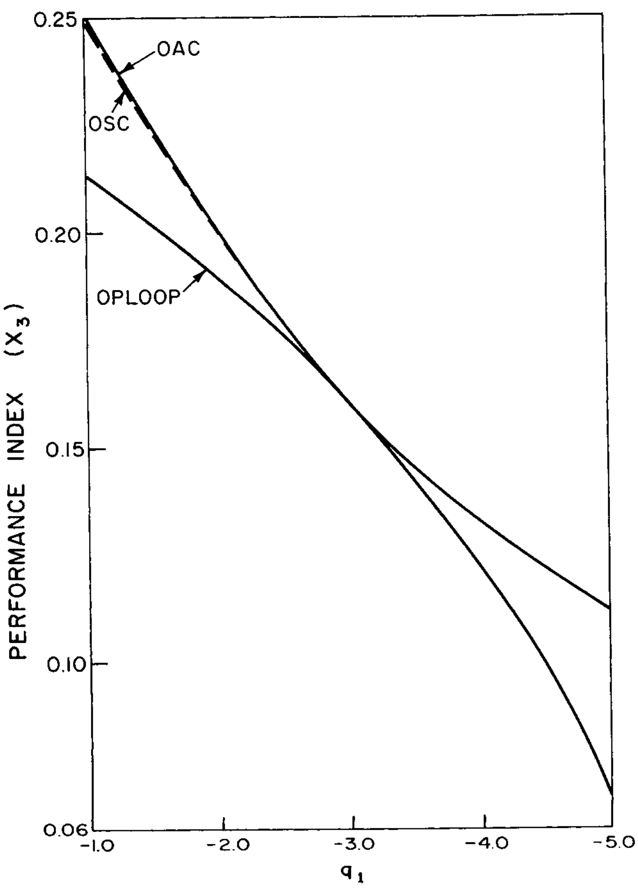

Fig. 7. Performance index of biochemical reactor versus parameter q_1. $q_2^* = -1.0$.

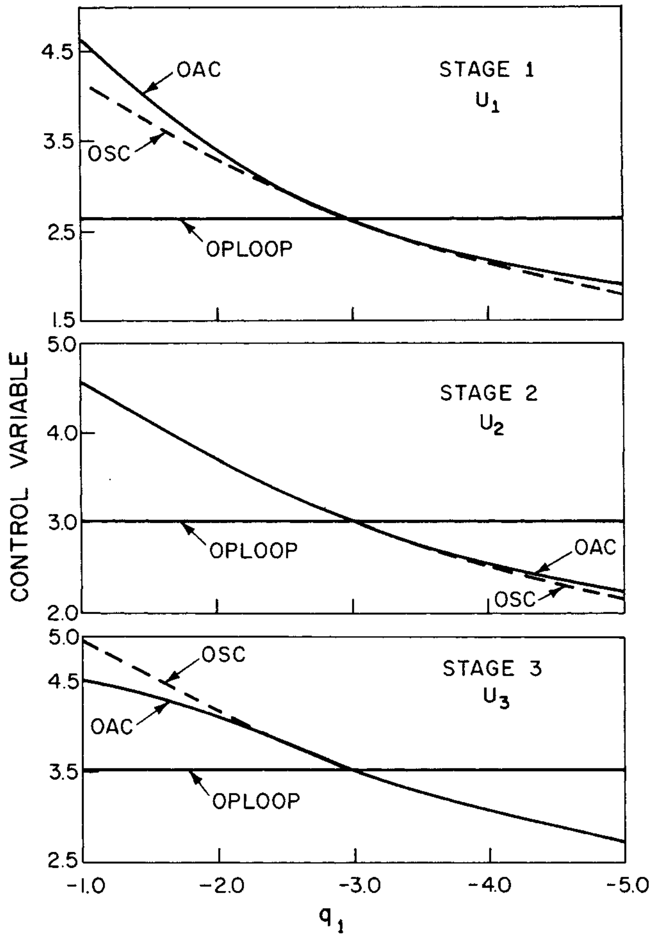

Fig. 8. Control policy of biochemical reactor for variations of parameter q_1. $q_2^* = -1.0$.

TABLE 2. RANGE OF SINGLE-PARAMETER VARIATIONS OF BIOCHEMICAL REACTOR FOR WHICH OSC CAN COMPENSATE

Parameter	Nominal value	Range
q_1	−3.0	$-5.0 \leq q_1 \leq -1.7$
q_2	−1.0	$-1.5 \leq q_2 \leq -0.5$
θ	.010	$.005 \leq \theta \leq .015$

(state x_3 is measured)

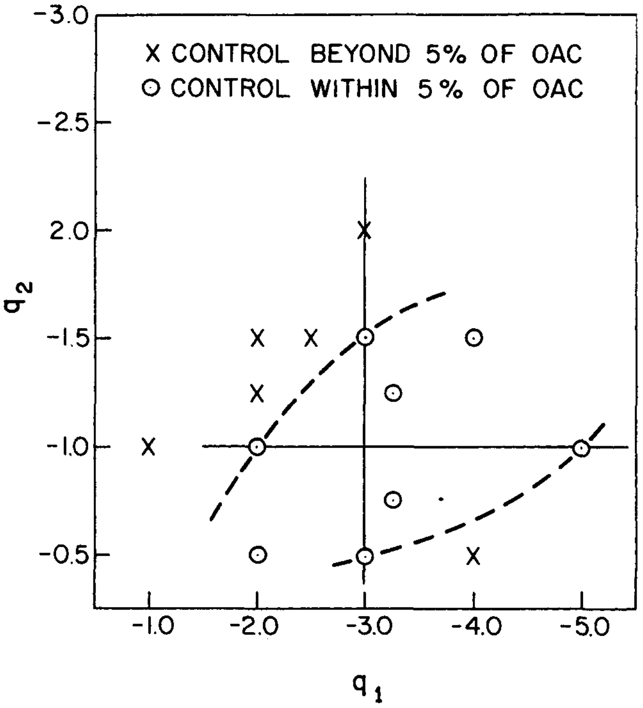

Fig. 9. Region in parameter space where OSC control policy matches OAC within 5%.

Thus, even where the controller is beyond the validity of its first-order approximations, and the generated control is not optimal, the penalty enacted as measured by the performance index is small. Here, we shall consider the range of validity of the controller as being the more conservative measure, where the generated control policy matches the OAC to within 5%. Using this criterion, the approximate range of single-parameter variations for which the controller can optimally compensate is presented in Table 2.

In compensating for dual-parameter variations, a minimum of two states must be examined. For this problem it makes no difference which two states are measured since there are only two independent state variations permissible. The third state will always be determined by the material balance relation

$$x_1(k) + x_2(k) + x_3(k) = x_1(0) + x_2(0) + x_3(0)$$

Instability was only noticed for simultaneous variations of q_1 and θ, and reduction of the feedback gain alleviated this difficulty. The domain of validity of the controller for these dual deviations is comparable to the corresponding range for single parameters. This is shown in Figure 9. Again, this range has been selected to where the OSC matches the optimally adaptive control within 5%.

CONCLUSIONS

Inclusion of sensitivity terms in the performance index is a feasible approach toward attaining sensitivity reduction. This approach does result however, in an increase in the performance index even if no parameter variations occur. If some or all the system states can be measured on-line, an optimally sensitive controller (OSC) would be preferable. For the continuous, discrete-time and discrete-staged examples illustrated here, it has been shown to be quite capable of providing adaptive control over a significant range of parameter variations.

ACKNOWLEDGMENT

The authors acknowledge the support of this work from National Science Foundation Grant NSF-GP-2858. Furthermore, this work made use of Princeton University computer facilities supported in part by National Science Foundation Grants NSF-GJ-34 and GU-3157.

NOTATION

$\mathbf{A}, \mathbf{B}$ = $(n \times n)$ and $(n \times m)$ matrices in state equation
$\overline{\mathbf{A}}, \overline{\mathbf{F}}$ = $(n + r) \times (n + r)$ matrices
d, h = rate constants
I = scalar performance index
$\mathbf{K}_{fb}$ = feedback matrix
m = dimension of control vector
n = dimension of state vector
N = total number of discrete time intervals over which a discrete system is controlled
$\mathbf{P}$ = matrix employed in Riccati transformation
q = scalar parameter
$\mathbf{q}$ = (r)-dimensional parameter vector
q_1, q_2 = first (second) element of parameter $\mathbf{q}$
$\mathbf{Q}, \mathbf{R}, \mathbf{S}$ = weighting matrices in performance index
$\overline{\mathbf{Q}}$ = combined weighting matrix of $\mathbf{Q}$, $\mathbf{Q}_1$, and $\mathbf{Q}_2$ for open-loop sensitivity reduction
$\mathbf{Q}_1, \mathbf{Q}_2$ = weighting matrix for sensitivity vector $\boldsymbol{\sigma}_1$ and $\boldsymbol{\sigma}_2$
r = dimension of parameter vector
$\overline{\mathbf{S}}$ = combined weighting matrix of $\mathbf{S}$, $\mathbf{S}_1$, and $\mathbf{S}_2$
$\mathbf{S}_1, \mathbf{S}_2$ = weighting matrix for $\boldsymbol{\sigma}_1$ and $\boldsymbol{\sigma}_2$ at terminal time
t = independent variable, time
t_f = terminal time
$\mathbf{u}, \mathbf{v}$ = control vector of dimension m
$\mathbf{u}_\mathbf{q}, \mathbf{x}_\mathbf{q}$ = partial derivative of $\mathbf{u}$ and $\mathbf{x}$ with respect to $\mathbf{q}$
$\mathbf{x}$ = state vector of dimension n
$\mathbf{X}, \mathbf{Y}$ = $(n + r)$-dimensional vector formed from $\mathbf{x}$ and $\mathbf{q}$

Greek Letters

$\boldsymbol{\eta}$ = adjoint sensitivity matrix to initial conditions
Δ = deviation of a quantity from nominal
$\boldsymbol{\Delta}$ = integral exponential matrix
θ = residence time parameter
$\boldsymbol{\lambda}$ = $(n + r)$-dimensional adjoint vector
λ = maximum eigenvalue of overall closed-loop matrix
$\boldsymbol{\nu}$ = control sensitivity matrix to initial conditions
$\boldsymbol{\xi}$ = state sensitivity matrix to initial conditions
$\boldsymbol{\sigma}$ = $(n \times r)$-dimensional state sensitivity matrix
$\boldsymbol{\varphi}$ = exponential matrix
ω = numerical value for element (1, 1) of the weighting matrix $\mathbf{Q}_1$
$\wedge$ = measured quantity
$*$ = quantity evaluated along nominal (undeviated) trajectory

LITERATURE CITED

1. Athans, M., and P. L. Falb, "Optimal Control," McGraw-Hill, New York (1966).
2. Barnett, S., *Intern. J. Control.*, 4, 41 (1966).
3. *Ibid.*, 10, 665 (1969).
4. Bradt, A. J., *IEEE Trans. Auto. Control*, 13, 110 (1968).
5. Breakwell, J. V., J. I. Speyer, and A. E. Bryson, *J. SIAM Control*, 1, 193 (1963).
6. Chang, T. M., and C. Y. Wen, *Ind. Eng. Chem. Fundamentals*, 7, 422 (1968).
7. D'Angelo, H., M. L. Moe, and T. C. Hendricks, *Proc. 4th Allerton Conf.*, 489 (1966).
8. Fan, L., and C. Wang, "The Discrete Maximum Principle," Wiley, New York (1964).

9. Kokotovic, P. V., J. B. Cruz, et al., *IEEE Proc.*, **56**, 1318 (1968).
10. Kriendler, F., *Grumman Aircraft Tech. Rept.*, AFFDL-TR-66-209 (Apr. 1967).
11. ———, *Intern. J. Control*, **2**, 171 (1967).
12. ———, *J. Franklin Inst.*, **285**, 26 (1968).
13. ———, *IEEE Trans. Auto. Control*, **13**, 254 (1968).
14. ———, *Intern. J. Control*, **8**, 89 (1968).
15. Lapidus, L., and R. Luus, "Optimal Control of Engineering Processes, Blaisdell, Waltham, Mass. (1967).
16. Lee, E. S., *Ind. Eng. Chem. Fundamentals*, **3**, 373 (1964).
17. McClamroch, N. H., and J. K. Aggarwal, *Proc. 5th Allerton Conf.* (Oct. 1967).
18. ———, *J. Franklin Inst.*, **285**, 483 (1968).
19. Pagurek, B., *Intern. J. Control*, **1**, 33 (1965).
20. ———, *IEEE Trans. Auto. Control*, **10**, 178 (1965).
21. Pontryagin, L. S., et al., "The Mathematical Theory of Optimal Processes," Interscience, New York (1962).
22. Rissanen, J. J., and R. Durbeck, *J. Basic Eng.*, **89**, 311 (1967).
23. ———, *IEEE Trans. Auto. Control*, **11**, 530 (1966).
24. Rohrer, R. A., and M. Sobral, *ibid.*, **10**, 43 (1965).
25. Sage, A. P., "Optimum Systems Control," Prentice-Hall, Englewood Cliffs, N.J. (1968).
26. Seinfeld, J. H., *AIChE J.*, **15**, 57 (1969).
27. ———, *Can. J. Chem. Eng.*, **47**, 212 (1969).
28. Sobral, M., *IEEE Proc.*, **56**, 1644 (1968).
29. Tomovic, R., "Sensitivity Analysis of Dynamic Systems," McGraw-Hill, New York (1963).
30. Weinrich, S. D., Ph.D. dissertation, Princeton Univ., (Sept. 1970).
31. Werner, R. A., and J. E. Cruz, *IEEE Trans. Auto. Control*, **13**, 621 (1968).
32. Witsenhausen, H. S., *ibid.*, **10**, 495 (1965).
33. *Ibid.*, **11**, 620 (1966).

Manuscript received November 24, 1970; revision received March 18, 1971; paper accepted March 19, 1971.

Entrance Region Flow of Polymer Melts

CHANG DAE HAN

Department of Chemical Engineering

Polytechnic Institute of Brooklyn, Brooklyn, New York 11201

An experimental study has been made to investigate polymer melt flow in the entrance region of a circular tube. For the study, a capillary rheometer was used to measure wall normal stresses in polymer melts in the reservoir and along the axis of the capillary. In order to investigate the influence of reservoir diameter on the entrance pressure drops, reservoir-to-capillary diameter (D_R/D) ratios of 3, 6, 9, and 12 were used, with the capillary length-to-diameter (L/D) ratio being 20 and the capillary diameter being 0.125 in. Analysis of the experimental data shows that the entrance pressure drop increases and then levels off as D_R/D ratio is increased. A correlation between the dimensionless entrance pressure drop and Reynolds number has been obtained, which follows the creeping flow analysis by Weissberg over the range of the area contraction ratio studied, $0.00694 \leq \beta \leq 0.111$.

When fluid enters a tube from a large reservoir, the velocity profile starts to develop and continues to change until a certain distance is reached beyond which flow is said to be fully developed. The finite length of tube required for attaining a fully developed flow profile is known as the entrance length. Clearly, the magnitude of the entrance length is dependent upon the viscosity of the fluid, the diameters of the tube and the reservoir, velocity of the fluid (for Newtonian fluids), and the elastic properties (for viscoelastic fluids). The criterion for determining fully developed flow in viscoelastic fluids (for example, polymer melts) has been a controversial subject. A conventional criterion, such as the constant pressure gradient in the tube, does not seem sufficient, although necessary, for viscoelastic fluids, while of course the same criterion has been well accepted for Newtonian fluids. Conditions other than the constant pressure gradient in polymer melt flow have recently been suggested by Han and Charles (*1*).

As one may surmise, the entrance length problem is intimately related to the flow situation in the reservoir. It is a well-established fact that viscoelastic fluids start to build their streamline in the reservoir before they actually reach the entrance of the tube. It has also been known for a long time that when viscoelastic fluids, in particular polymer melts, flow from a reservoir into a circular tube, they undergo excessively large pressure drops. This pressure drop is considerably greater for polymer melts than for Newtonian fluids. There is ample evidence that the viscosity of the material alone cannot explain such excessive pressure drops. And some efforts (*2* to *4*) have been made to explain the excessive pressure drops of polymer melts in terms of the elastic properties of the material.

In the past, attempts have been made by several investigators (*5* to *8*) to relate the entrance pressure drops (or the entrance lengths) theoretically both to the rheological properties of non-Newtonian fluids and to the geometries of the reservoir and tube as well. Invariably these investigators approached the problem by means of boundary-layer analysis. However, applicability of their analyses to polymer melt flow in the entrance region is highly questionable, because in most flow situations of practical interest, polymer melts yield exceedingly low Reynolds num-